Journal of Crystal Growth 101 (1990) 246–250
North-Holland

TWINNING IN CdTe

K. DUROSE and G.J. RUSSELL

Applied Physics Group, School of Engineering and Applied Science, University of Durham, South Road, Durham DH1 3LE, UK

The crystallography of twins in the sphalerite structure is reviewed and coincidence site lattice models of first and second order twin boundaries are presented. These models predict the indices of the boundary planes of twins and give an indication of their atomic structure. Observations of twins in bulk crystals of vapour-grown CdTe made by chemical etching and TEM are also reported upon.

1. The importance of twins in CdTe

The incidence of twinning in bulk crystals of CdTe grown by all techniques is a generally acknowledged problem [1]. Twinned regions of a crystal have a different but defined crystallographic orientation to that of their host lattice and as such are special cases of grains boundaries [2]. Twinning in CdTe presents problems on two accounts. Firstly if twinned crystals are used as substrates for epitaxy the orientation differences are propagated into the epilayer [3]. Secondly, CdTe [4] and (CdHg)Te [5] grown epitaxially on single grained {111} oriented substrates contain thin lamellar twins lying parallel to the epitaxial interface.

In this work, we use coincidence site lattice (CSL) models to give a primary indication of twin boundary structure. We also report on the incidence of twinning in bulk CdTe crystals grown from the vapour in sealed capsules [6].

2. The crystallography of twinning

The relationship of a first order twin to its host lattice is variously described as: (a) a change in the stacking sequence of {111} planes in the twin respective to the host lattice [7,8], (b) a rotation of the twin with respect of the host lattice by 180°C about a ⟨111⟩ twist axis [9,10], or (c) a rotation of the twin with respect to the host by either $\theta = 70° 32'$ or $\Theta = 250° 32'$ about a ⟨110⟩ tilt axis [11].

The two possible rotation angles indicated in the latter are indistinguishable in diamond but differ in sphalerite [11] due to its noncentrosymmetric nature-and are known as "para" and "ortho" types respectively. Only the low energy "ortho" boundary equivalent to b above (in which all bonding opportunities can be satisfied for a mutual {111} interfacial plane) is found in practice [10,12,13]. The low interfacial energy associated with these so called coherent twin boundaries lying on {111} accounts for the high incidence and straightness of first order twin bands in bulk CdTe [14]. Interfaces lying on other planes which terminate twin lamellae are known as lateral or incoherent twin boundaries and these have higher interfacial energies [15]. Twin orientations can exist within grains which are already twinned once or more with respect to the host lattice and these are referred to as second and higher order twins, the direct interfaces between them and the host being second and higher order twin boundaries. Relationships between the orientations of host and twinned grains in sliced boules are of great practical importance and may be calculated with reference to a simple matrix method [16,17]. The surface orientations of twinned grains have also been tabulated by Slawson [18].

0022-0248/90/$03.50

3. Coincidence site lattice models of twin boundaries in the sphalerite lattice

An alternative description of twinning relationships was derived by Ellis and Treuting [19] using the concept of the coincidence site lattice (CSL). The CSL may be derived by superimposing the lattices of two adjacent grains and choosing those points common to both. The ratio of CSL points to lattice points is the Friedel index Σ [20]. All first and higher (Nth) order twins in the diamond lattice may be described as tilts about $\langle 110 \rangle$ axes having Friedel indices of $\Sigma = 3^N$. Kohn [21] used the CSL concept to derive the indices of the interfacial planes of $\Sigma = 3$, 9 and 27 boundaries in the diamond lattice. Low energy interfaces were identified as lying on planes having high densities of reciprocal lattice points. Once identified on the CSL, addition of the twin and host lattices on either side of the boundaries allowed the positions of possible bonds at the interfaces to be inserted.

The procedure used by Kohn has been adopted by the present authors for the sphalerite lattice in the analysis of $\Sigma = 3$ [15] and $\Sigma = 9$ boundaries. In the case of the first order twin it is possible to generate two $\langle 110 \rangle$ projections of CSLs corresponding to tilt angles about that axis of $\theta = 70°\ 32'$ and $\Theta = 250°\ 32'$, that is, the "para" and "ortho" twins. However, the "para" twinning CSL contains only half the density of CSL points found in that for "ortho" twinning, hence providing another basis upon which to use the CSL for the (experimentally confirmed) "ortho" twin. Similarly, for the second order twin a tilt angle of $\Theta = 218°\ 57'$ about $\langle 110 \rangle$ represents a $\Sigma = 9$ boundary having twice the density of CSL points

Table 1
Interfacial planes of $\Sigma = 3$ and $\Sigma = 9$ boundaries in the sphalerite lattice indexed with respect to both the host and twin orientations; an explanation of the CSL atomic locations is given in table 2

$\Sigma = 3$ (first order) boundary planes	CSL atomic locations present	$\Sigma = 9$ (second order) boundary planes	CSL atomic locations present
{111}–{111} coherent	c	{111}–{115}	a, a′, b
{115}–{111}	a, a′, b	{114}–{114}	a, a′, b
{112}–{112} lateral	a, a′, b	{211}–{211}	b, d
{001}–{221} or	a, a′, b, c		
{110}–{114} incoherent	a, a′, b, c		

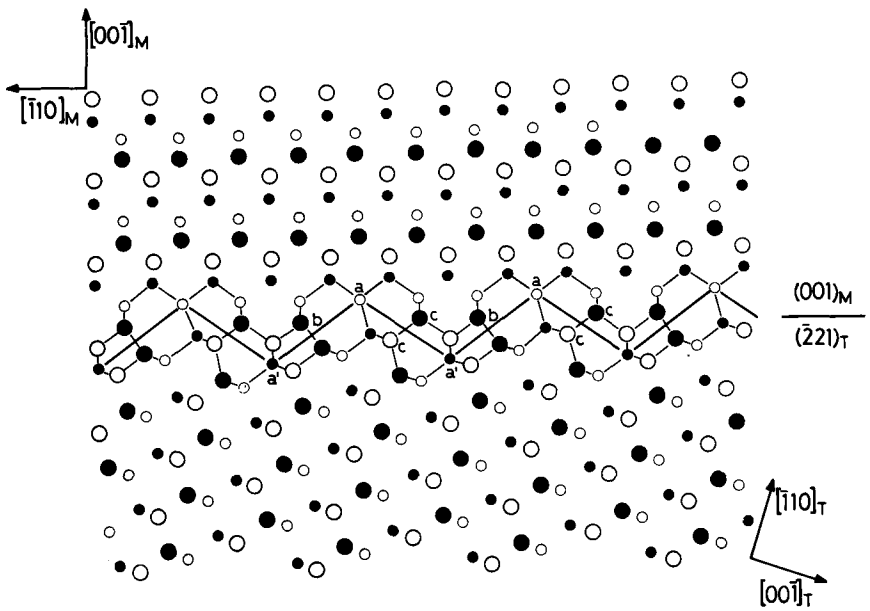

Fig. 1. CSL model of a $\Sigma = 3$ (first order twin) boundary lying on the planes {001}–{221}.

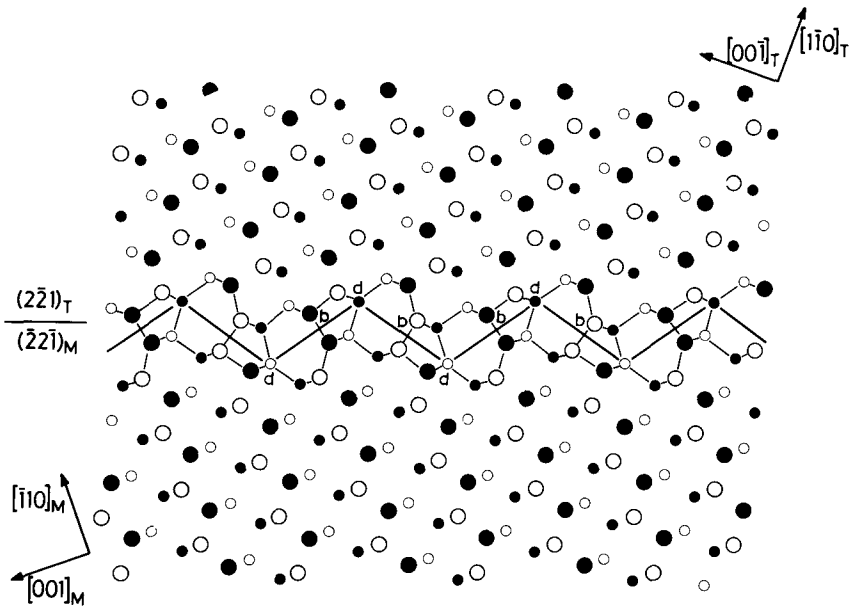

Fig. 2. CSL model of a $\Sigma = 9$ (second order twin) boundary lying on the planes {221}–{221}.

of the polarity inverted $\theta = 38°\ 57'$ boundary. Table 1 lists the indices of the interfacial planes of $\Sigma = 3$ and $\Sigma = 9$ boundaries predicted using the two "high density" CSLs.

Examples of reconstructed atomic bonding configurations at the {001}–{221} first order lateral and {221}–{221} second order twin boundaries are shown in figs. 1 and 2 respectively. Characteristic bonding sites recur in both $\Sigma = 3$ and $\Sigma = 9$ boundaries and these are listed in table 2. These include wrongly coordinated atoms (a and a′) and wrong bonds (b), in addition to 4-coordinated atoms having distorted tetrahedral bonding (d). Some of these bonding sites would undoubtedly act as centres for electron–hole pair recombination and hence be associated with deleterious electrical activity. Pure CSL representations of the boundaries do not however, take into account atomic relaxations and the rigid body shifts between the twins and their hosts which could take place to minimise the free energies of the boundaries. Such changes have been considered by Pond [22] for $\Sigma = 3$ boundaries in Si and, by analogy, for the sphalerite lattice by Durose and Russell [15]. It is apparent that without corroboration from direct observations of the structure of twin boundaries by HRTEM it is only possible to use CSLs to indicate in general terms the types of defect sites present at twin interfaces.

4. Direct observations of twin boundaries in CdTe crystals

4.1. Indexing of twin boundaries

Over 100 boules of CdTe have been grown in these laboratories from the vapour phase [6] and this material has been characterized by chemical etching with Nakagawa's reagent [23], Inoue's reagents [10,24], a 0.5% solution of bromine in methanol in the presence of illumination [17] and also by CTEM. All the boules were twinned on at least one set of {111} planes while many were comprised entirely of first and higher order twinned grains. Indexing of the lateral and higher order boundaries was achieved by etching oriented surfaces and measuring the angles of intersection of these boundaries with coherent ones on {111}. An example is shown in fig. 3 in which a first order twin band (a) intersecting a Cd {111} surface is terminated by a {110}–{114} lateral twin

Table 2
Atomic locations in CSL models of $\Sigma = 3$ and $\Sigma = 9$ boundaries

a	Three coordinated atoms having one bond rotated into the plane of the figure by 57° 1′
a′	Five coordinated atoms having one bond rotated out of the plane of the figure by 57° 1′; two of the nearest neighbours of such atoms are not in the planes represented in the figures
b	The site of a Te–Te or Cd–Cd wrong bond; the bonds from both atoms in the equivalent diamond structure are rotated by 19° 81′ in the plane of the figure and are approximately 6% shorter than normal
c	Four coordinated atoms with normal undistorted tetrahedral bonding
d	Tetrahedrally coordinated atoms with distorted bonding

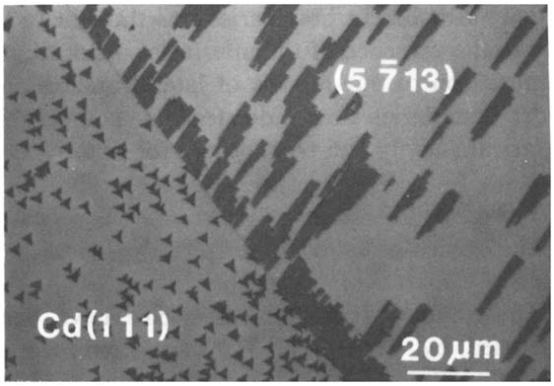

Fig. 4. Second order twin boundary lying on {114}–{114} etched with Inoue's EAg-1 reagent [10].

boundary (b). Indexing was also carried out using the crystallographic facets of Inoue EAg-1 etch pits [10,17,25] as reference directions. Fig. 4 shows a {114}–{114} second order twin boundary separating the {111} and {5$\bar{7}$13} orientations of a slice etched with EAg-1. Using these methods, all of the first and second order twin boundary planes predicted by the CSL models and listed in table 1 were identified. No others were observed.

4.2. Defects and electrical activity at twin boundaries

The incidence of Te precipitates in this vapour grown material has been established by etching and SEM/EDAX. Precipitates in this material are ~ 10 μm in width and are more frequently seen in association with boundaries than in the bulk material. Furthermore, the number of precipitates decorating a unit length of a boundary decreases according to the sequence; non-crystallographic random grain boundary > second order twin boundary > first order lateral twin boundary > first order coherent twin boundary [26]. This sequence presumably reflects the decreasing free energies of these boundaries and the lower free energy reductions associated with precipitation at the more ordered boundaries [27]. This explanation is probable, since crystal growth by the sealed capsule technique used is slow and entails maintaining the boules at high temperature for several days allowing energetically favourable distributions of precipitates to become established.

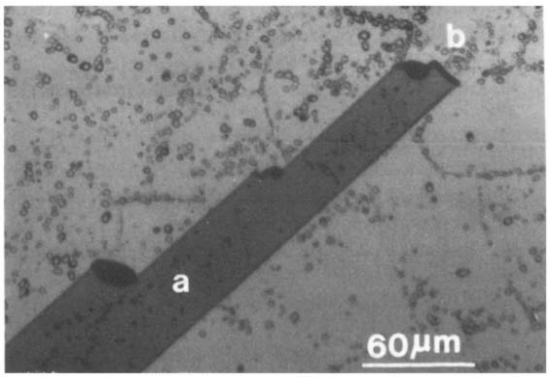

Fig. 3. First order twin band (a) intersecting a {111} Cd surface and terminated by a lateral twin boundary (b) lying on the planes {110}–{114}. Etched with Nakagawa's reagent [23].

Our TEM studies of first order coherent twin boundaries have revealed dislocations lying on the interfacial planes themselves [14,17,28]. We have not identified the Burgers vectors of these dislocations but they must be either $\frac{1}{6}\langle 211\rangle$ type partials (i.e. twinning dislocations) or else result from some growth phenomenon, possibly the migration of dislocations followed by pinning at the boundary.

An earlier EBIC investigation by the authors [15] indicated that both lateral and coherent boundaries are electrically active. The high density of recombination centres in the former was attributed to interfacial bonding defects, while residual

activity at coherent boundaries was thought to be due to the presence of the interfacial dislocations. Comparison of our models of lateral and second order boundaries now indicates that comparable electrical activity can be expected for both.

5. The origins of twinning in CdTe

The origins of twinning in CdTe have been discussed by Vere et al. [1] who attempted to induce twinning in CdTe by applying stress to ⟨123⟩ oriented bars at elevated temperatures. This experiment induced no twins, a result expected by Aindow [29] who indicates that the flow stress required to promote deformation twinning by a dislocation mechanism would be far in excess of the stress supported by the materials before the onset of slip. Furthermore, even though dislocations are observed on the twin boundaries themselves (see above) their origin is by no means clear and there is no evidence in CdTe of the incidence of the lenticular twin grains which are characteristic of deformation twinning in metals.

A more likely formation mechanism is via growth accidents either on {111} or {211} for example, the latter having been recorded recently in Si by HRTEM [30].

References

[1] A.W. Vere, S. Cole and D.J. Williams, J. Electron. Mater. 12 (1983) 551.
[2] K.T. Aust and J.W. Rutter, Trans. Met. Soc. AIME 215 (1959) 820.
[3] G.R. Awan, A.W. Brinkman, G.J. Russell and J. Woods, J. Crystal Growth 85 (1987) 477.
[4] P.D. Brown, J.E. Hails, G.J. Russell and J. Woods, J. Crystal Growth 86 (1988) 511.
[5] J. Hails, G.J. Russell, P.D. Brown, A.W. Brinkman and J. Woods, J. Crystal Growth 86 (1988) 516.
[6] G.J. Russell, N.F. Thompson and J. Woods, J. Crystal Growth 71 (1985) 621.
[7] G. Aminoff and B. Broome, Z. Krist. Mineral. (Leipzig) 80 (1931) 335.
[8] J.R. Cutter, G.J. Russell and J. Woods, J. Crystal Growth 32 (1976) 179.
[9] K. Zanio, in: Semiconductors and Semimetals, Vol. 13, Cadmium Telluride, Eds. R.K. Willardson and A.C. Beer (Academic Press, New York, 1978).
[10] M. Inoue, I. Teramoto and S. Takayanagi, J. Appl. Phys. 33 (1962) 2578.
[11] D.B. Holt, J. Phys. Chem. Solids 30 (1969) 1297.
[12] K. Durose, G.J. Russell and J. Woods, in: Microscopy of Semiconducting Materials 1985, Inst. Phys. Conf. Ser. 76, Eds. A.G. Cullis and D.B. Holt (Inst. Phys., London–Bristol, 1985) p 233.
[13] H. Iwanaga, N. Shibata, A. Tanaka and Y. Masa, J. Crystal Growth 84 (1987) 345.
[14] K. Durose, G.J. Russell and J. Woods, J. Crystal Growth 72 (1985) 85.
[15] K. Durose and G.J. Russell, in: Microscopy of Semiconducting Materials 1987, Inst. Phys. Conf. Ser. 87, Eds. A.G. Cullis and P.D. Augustus (Inst. Phys., London–Bristol, 1987) p. 327.
[16] K.F. Hulme and J.B. Mullin, Solid State Electron. 5 (1962) 211.
[17] K. Durose, Structural Defects in CdTe, PhD Thesis, University of Durham (1986).
[18] C.B. Slawson, Am. Mineralogist 35 (1950) 193.
[19] W.C. Ellis and R.G. Treuting, J. Metals 3 (1951) 53.
[20] An earlier independent derivation of the CSL concept is described in the French language by G. Friedel, Leçons de Cristallographie (Berger Levrault, Paris, 1926).
[21] J.A. Kohn, Am. Mineralogist 43 (1958) 263.
[22] R.C. Pond, J. Physique Colloq. 43 (1982) C1–51;
R.C. Pond, D.J. Bacon and A.M. Bastaweesy. in: Microscopy of Semiconducting Materials 1983, Inst, Phys. Conf. Ser. 67, Eds. A.G. Cullis, S. M. Davidson and G.R. Booker (Inst. Phys., London–Bristol, 1983) p. 253.
[23] K. Nakagawa, K. Maeda and S. Takeuchi, Appl. Phys. Letters 34 (1979) 574.
[24] M. Inoue, I. Teramoto and S. Takayanagi, J. Appl. Phys. 34 (1963) 404.
[25] H. Iwanaga, T. Yoshiie, S. Takeuchi and K. Mochizuki, J. Crystal Growth 61 (1983) 691;
H. Iwanaga, A. Tomizuka, N. Shibata and K. Mochizuki, J. Crystal Growth 74 (1986) 113.
[26] K. Durose and G.J. Russell, J. Crystal Growth 86 (1988) 471.
[27] H. Gleiter, Acta Met. 18 (1970) 117.
[28] P.D. Brown, Structural Defects in II–VI Epitaxial Layers, PhD Thesis, University of Durham (1988).
[29] M. Aindow, private communication.
[30] R. Sinclair et al., in: Microscopy of Semiconducting Materials 1989, Inst. Phys. Conf. Ser., Eds. A.G. Cullis and J.L. Hutchison (Inst. Phys., London–Bristol, 1989).